

Electrochemical performance of polyaniline nanofibres and polyaniline/multi-walled carbon nanotube composite as an electrode material for aqueous redox supercapacitors

S.R. Sivakkumar^a, Wan Ju Kim^a, Ji-Ae Choi^a, Douglas R. MacFarlane^b,
Maria Forsyth^c, Dong-Won Kim^{a,*}

^a Department of Applied Chemistry, Hanbat National University, Yuseong-Gu, Daejeon 305-719, Republic of Korea

^b School of Chemistry, Monash University, Wellington Road, Clayton, Vic. 3800, Australia

^c Department of Materials Engineering, Monash University, Wellington Road, Clayton, Vic. 3800, Australia

Received 4 April 2007; received in revised form 7 May 2007; accepted 29 May 2007

Available online 19 June 2007

Abstract

Polyaniline (PANI) nanofibres are synthesized by interfacial polymerization and their electrochemical performance is evaluated in an aqueous redox supercapacitor constituted as a two-electrode cell. The initial specific capacitance of the cell is 554 F g^{-1} at a constant current of 1.0 A g^{-1} , but this value rapidly decreases on continuous cycling. In order to improve the cycleability of the supercapacitor, a composite of polyaniline with multi-walled carbon nanotubes (CNTs) is synthesized by *in situ* chemical polymerization. Its capacitive behaviour is evaluated in a similar cell configuration. A high initial specific capacitance of 606 F g^{-1} is obtained with good retention on cycling. In both supercapacitors, the effect of charging potential on cycling performances is investigated.

© 2007 Elsevier B.V. All rights reserved.

Keywords: Carbon nanotube; Composite electrode; Electrochemical capacitor; Polyaniline; Redox supercapacitor

1. Introduction

High-surface carbons, noble metal oxides and conducting polymers are the main families of electrode materials being studied for supercapacitor applications [1,2]. Among them, ruthenium oxide and conducting polymers have been shown to deliver higher specific capacitance than carbon materials, since they store charge through both double-layer and redox capacitive mechanisms. Porous carbon materials can also present a pseudo-capacitive behaviour due to redox processes undergone by adsorbed surface functionalities, but the contribution of the surface groups to the total charge storage is not as important as the one related to the double-layer charge. Since conducting polymers offer the advantages of lower cost compared with ruthenium oxide, they have been paid much attention as electrode materials. A wide variety of conduct-

ing polymers such as polyaniline [3–8], polypyrrole [9,10], poly(ethylenedioxythiophene) [11,12], polythiophene and its substituted counterparts [13,14] have been studied for supercapacitor applications. Of these, polyaniline (PANI) has been most actively investigated due to its low cost, ease of synthesis, high conductivity and stability.

Over the last decade, there have been many reports published on the use of polyaniline as an electrode material in both aqueous [15–17] and non-aqueous redox supercapacitors [18–20]. For this application, it is desirable to synthesize the polyaniline with high surface area. Higher surface area produces higher charge storage ability through both the double-layer mechanism and also the effective access of the electrolyte to the electrode in the redox mechanism. In this study, we have synthesized polyaniline nanofibres with high surface area and have evaluated their electrochemical performances as electrode materials in an aqueous redox supercapacitor. With the aim of improving the cycleability of the polyaniline electrode, a composite of polyaniline with multi-walled carbon nanotubes (CNT) is also synthesized and tested for its charge storage capability. The

* Corresponding author. Tel.: +82 42 821 1550; fax: +82 42 822 1562.

E-mail address: dwkim@hanbat.ac.kr (D.-W. Kim).

effect of charging potential on the cycling performance of the cells is also investigated.

2. Experimental

2.1. Preparation of PANI nanofibre-based electrodes

Polyaniline nanofibres were synthesized by interfacial polymerization as reported in the literature [21], which is briefly described as follows. Aniline was dissolved at a concentration of 0.5 M in 500 ml of CH_2Cl_2 . Ammonium persulfate was dissolved in 1.0 M HClO_4 solution. This aqueous solution was carefully spread over the organic solution that contained the aniline monomer and kept undisturbed at 25 °C for 24 h. This solution was filtered, and then washed with copious amounts of water and acetonitrile until the filtrate became colourless. Doping and de-doping was achieved by stirring the polymer in 1.0 M HClO_4 and 0.5 M NH_4OH , respectively, and then the product was filtered and vacuum dried. To prepare the electrodes, the de-doped (emeraldine base, EB form) polyaniline nanofibres (70 wt.%) were mixed with super-p (20 wt.%) as a conducting material and with carboxy methyl cellulose (CMC) (6 wt.%) and styrene-butadiene rubber (SBR) (4 wt.%) as a binder in an aqueous medium. The mixture was ball-milled for 15 h and then the resultant slurry was cast on Ti foil (55- μm thick) to a thickness of 70 μm by means of a doctor blade. The electrodes were dried in a vacuum oven and roll-pressed to enhance particulate contact and adhesion to the foils. The thickness of the polymer coated on Ti foil after roll-pressing was about 30 μm .

2.2. Preparation of PANI/CNT composite-based electrodes

Multi-walled CNT was purchased from ILJIN Nanotech. It had been prepared by a chemical vapour deposition process and its aspect ratio was about 1000. The PANI/CNT composite was prepared by adopting the *in situ* chemical synthesis method. CNT was suspended in 1.0 M HClO_4 solution containing aniline monomer. This suspension was sonicated for 3 h, to facilitate the good dispersion of CNT. After sonication, the solution was transferred to a polymerization reactor and cooled to 1 °C. A 1.0 M HClO_4 solution containing ammonium persulfate was then added drop-by-drop for 1 h, with mechanical stirring of the monomer solution at 300 rpm. After stirring for 3 h, the temperature was increased to 15 °C and stirring continued overnight. In order to investigate the effect of sonication in the synthesis of the PANI/CNT composite, another similar synthesis was carried out without sonication. The nanocomposite materials were then filtered, washed with water and acetonitrile, and then vacuum dried for 24 h. De-doping was achieved by stirring the nanocomposites in 0.5 M NH_4OH . From the weight of the de-doped material (EB form), the ratio of PANI and CNT was calculated to be 74:26 (w/w), respectively. The EB form of the composite material (90 wt.%) was mixed with CMC (6 wt.%) and SBR (4 wt.%) as binder in aqueous medium. Electrodes were prepared via the same procedure adopted for the polyaniline nanofibre electrodes.

2.3. Cell assembly and measurements

Sandwich-type cells were assembled with two symmetric polyaniline nanofibre electrodes or PANI/CNT composite electrodes (area: 2 cm \times 2 cm). The electrolyte used in assembling the cell was 1.0 M H_2SO_4 with a microporous polyethylene-polypropylene separator. The electrodes and separator were soaked in the electrolyte before cell assembly. The symmetrical cell was enclosed in a metallized plastic bag and vacuum-sealed. The morphologies of the polyaniline nanofibres and PANI/CNT composite were examined by means of a scanning electron microscope (PHILIPS, XL30SFEG). Cyclic voltammograms were recorded from 0 to 0.6 V at a scan rate of 10 mV s^{-1} . The AC impedance measurements were performed on a CH Instruments system in the frequency range of 0.01 Hz–100 kHz with an AC perturbation of 10 mV. Constant-current charge–discharge cycling of the cell was conducted over voltage ranges of 0–0.6 and 0–0.4 V at a current loading of 1.0 A g^{-1} with Toyo battery-test equipment (TOSCAT-3000U) at room temperature.

3. Results and discussion

3.1. Polyaniline nanofibre-based supercapacitors

Scanning electron micrographs of the polyaniline nanofibres are presented in Fig. 1. Morphological analysis of the polyaniline reveals a nanofibrous structure of fibres of diameter 90 nm and length 420 nm. The nanofibrous and porous morphology is thought to be desirable as an electrode material for redox supercapacitors, because it enables effective and rapid access of the electrolyte, which results in high charge storage and fast charge–discharge processes. As shown in Fig. 1(b), upon de-doping the polyaniline nanofibres, the diameter of the fibres is found to be slightly increased, as is the case with conventional polyaniline.

A sandwich-type cell was assembled using polyaniline nanofibres and 1.0 M H_2SO_4 . It was subjected to constant-current charge–discharge cycling tests at a current loading of 1.0 A g^{-1} in the voltage range of 0–0.6 V. Charge–discharge curves of the cell are presented in Fig. 2(a). Both charging and discharging times rapidly decrease on cycling, which indicates a rapid decrease in specific capacitance. A large IR drop can be also seen in the discharge curves. The specific capacitance of the electrode material was calculated using the formula of $C (\text{F g}^{-1}) = 2It/(m\Delta E)$, where I is the current applied for the charging and discharging, t the time of discharge, ΔE the voltage difference between the upper and lower potential limits and m is the mass of polyaniline in one of the electrodes. The factor of 2 arises from the fact that the total capacitance measured from the cell is the addition of two equivalent single electrode capacitors in series. Fig. 2(b) shows the specific capacitance and the Coulombic efficiency as a function of cycle number. In the initial cycle, the specific capacitance is 554 F g^{-1} , but rapidly decreases with cycling. At the 1000th cycle, the value is 57 F g^{-1} , which corresponds to 10% of the initial capacitance. The Coulombic efficiency of the cell is found to be nearly constant ($\sim 98\%$) throughout the entire cycle test. This

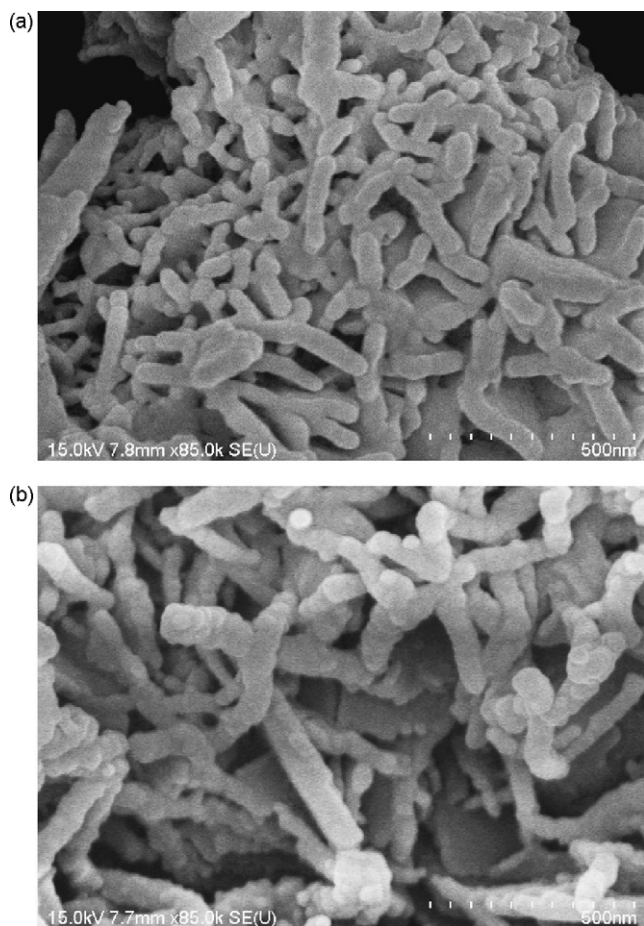


Fig. 1. Scanning electron micrographs of polyaniline nanofibres: (a) doped form and (b) de-doped form.

decrease in specific capacitance with cycling is in agreement with other studies on polyaniline-based redox supercapacitors [3,4,18–20]. Nonetheless, it should be noted that the polyaniline nanofibre-based cell delivers a very high initial capacitance, which is much greater than the values reported for conventional macroscopic polyaniline electrodes [3–5,16,18–20]. This higher specific capacitance is obviously due to the nanofibrous nature of the polyaniline yielding a higher surface area, which favours the effective access of the electrolyte and storage of more charge via both the double-layer and redox capacitive mechanisms. On the other hand, the amount of charge cycled in these devices is substantially less than the theoretical redox capacitance of the EB form of polyaniline (approximately 1767 F g^{-1} at 0.3 V per electrode). This form of polyaniline is capable of being both oxidized and reduced with this level of capacity in each direction. The fact that only a fraction (31%) of the theoretical capacitance is being utilized indicates that, in principle, the material is not being over oxidized or reduced, and also that the conductivity changes due to the change in state should not be significant. At the relatively high charge rates involved here (1 A g^{-1}), however, non-uniform distribution of the change in state may occur throughout the depth of the material, and thus cause the surface state to differ from the mean value.

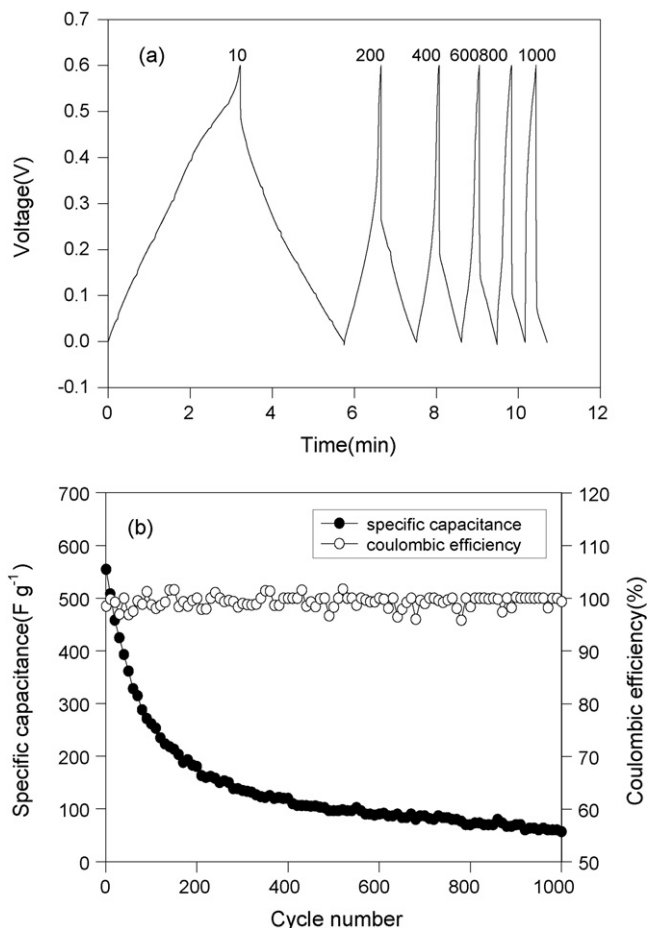


Fig. 2. Cycling performance of polyaniline nanofibre-based cell, which is cycled in the voltage range of 0–0.6 V at a current loading of 1.0 A g^{-1} . (a) Charge and discharge curves vs. time and (b) specific discharge capacitance and Coulombic efficiency vs. cycle number. Numbers in figure represent cycle number.

It is of interest to investigate how the cell performance is altered if the potential window is narrowed. Hence, cell testing was carried out in the voltage range of 0–0.4 V. The charge–discharge curves are presented in Fig. 3(a). The specific capacitance and Coulombic efficiency with cycle number are also plotted in Fig. 3(b). The specific capacitance of the cell on the first cycle is 292 F g^{-1} , which slowly increases to a maximum value of 339 F g^{-1} on the 110th cycle and then starts to decrease. On the 1000th cycle, the specific capacitance of the cell is 75 F g^{-1} , which corresponds to 26% of the initial capacitance. When comparing the capacitance retention in both 0.6 and 0.4 V cells, the latter proves to exhibit better cycleability than the 0.6 V cell. This result suggests that the cycleability of the redox supercapacitor assembled with polyaniline electrode can be improved by lowering the charging potential. Higher oxidation potentials may degrade the polyaniline electrode and result in a gradual loss of electroactivity and a decrease in specific capacitance. Additionally, the mechanical stress that is experienced by the polymer during doping and de-doping may have a strong effect on the properties of the electrode. As can be seen in Fig. 1, the diameter of the de-doped polyaniline fibres is increased in comparison with its doped form. When the polyaniline is repetitively cycled

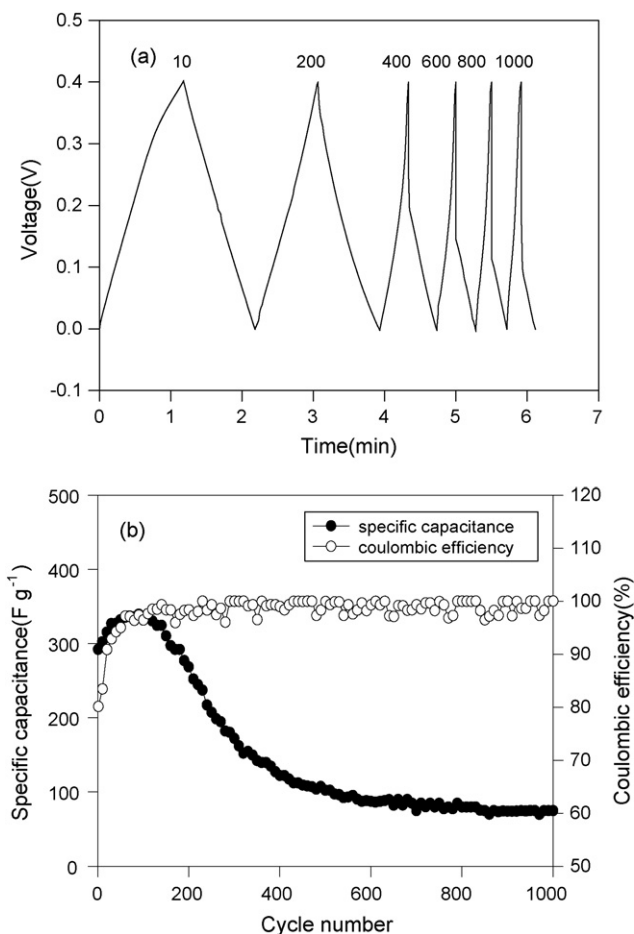


Fig. 3. Cycling performance of polyaniline nanofibre-based cell, which is cycled in the voltage range of 0–0.4 V at a current loading of 1.0 A g^{-1} . (a) Charge and discharge curves vs. time and (b) specific discharge capacitance and Coulombic efficiency vs. cycle number.

between its oxidized and reduced states, the material experiences repetitive swelling and shrinkage, which can cause mechanical stress to the polymeric backbone and gradually deteriorate the polymeric conductivity and charge storage capability. To examine further this effect, carbon nanotube composites of the PANI were formed in order to provide greater mechanical rigidity, as described further below.

3.2. Polyaniline/CNT composite-based supercapacitor

A composite of polyaniline with multi-walled carbon nanotubes was prepared and evaluated in an aqueous capacitor cell. CNTs have previously been shown to offer good mechanical support to polyaniline and thereby help to improve its cycleability in both supercapacitors and lithium batteries [22–27]. Moreover, the CNT ensures good electronic conduction in the electrode when the polymer is in an insulating state. The polyaniline/CNT composites were prepared using slightly different experimental conditions, i.e. with and without sonication, as discussed above in Section 2. The morphologies of the composite materials prepared with and without sonication are shown in Fig. 4(a and b), respectively. For comparison, the morphology of pure CNT used

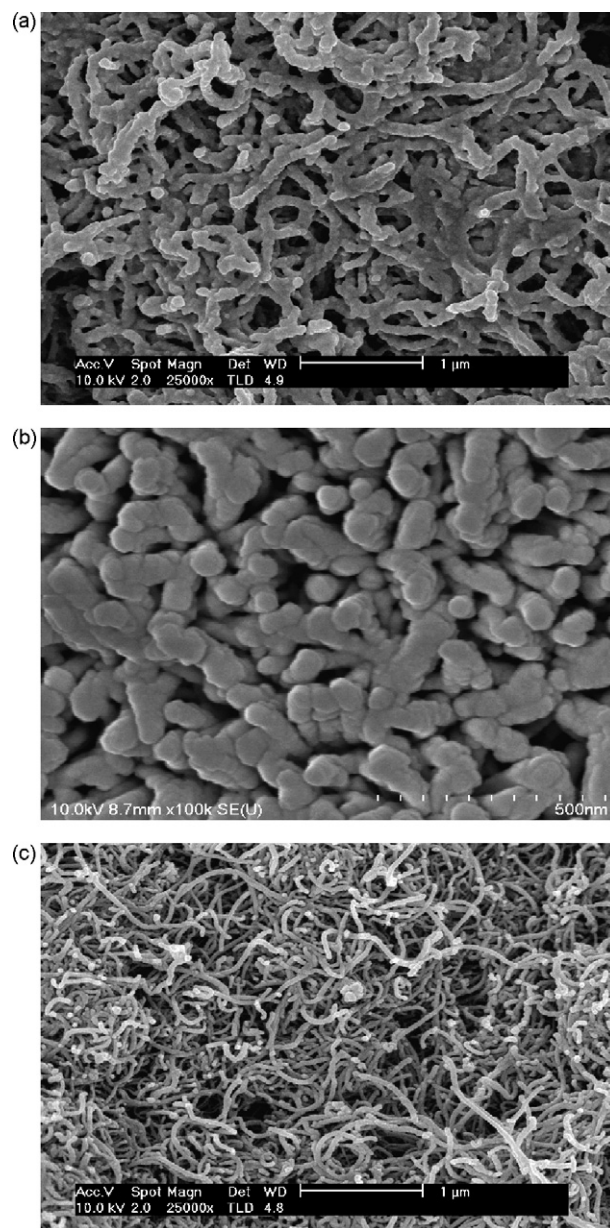


Fig. 4. Scanning electron micrographs of (a) PANI/CNT composite prepared with sonication, (b) PANI/CNT composite prepared without sonication and (c) pure CNT.

in the present study is also shown, in Fig. 4(c). From the images of CNT, the average diameter is measured to be about 40 nm. The PANI/CNT composites show an average diameter of 85 nm, which indicates that the CNTs are relatively evenly coated by the polyaniline layer. From Fig. 4(a), it can be observed that the composite prepared after sonication shows well-dispersed CNTs enwrapped uniformly with polyaniline. This highly interconnected and porous morphology is highly desirable for fast ion diffusion and migration in the electrodes. By contrast, the composite prepared without sonication contains bundles of CNTs coated with polyaniline. It consists of the tips of CNT coated with polyaniline in a particular bundle of CNT projecting perpendicular to the imaging direction. These results indicate the usefulness of sonication in preparing well-dispersed and highly

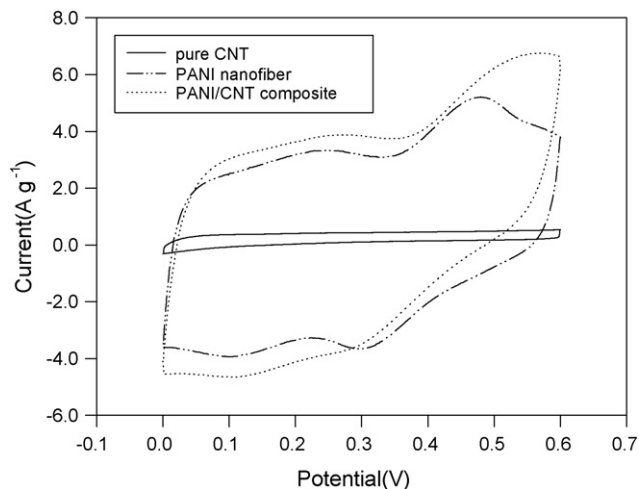


Fig. 5. Cyclic voltammograms for pure CNT, PANI nanofiber and PANI/CNT composite. Scan rate is 10 mV s^{-1} .

porous polyaniline/CNT composite material. Thus, in this study, the composite that was prepared with sonication is used.

A sandwich-type cell was assembled with the EB form of PANI/CNT composite and its capacitive behaviour was evaluated. Fig. 5 presents the cyclic voltammograms (CVs) for the PANI/CNT composite electrode-based cell, along with the CVs for pure CNT and PANI nanofiber cells. The CV of the pure CNT exhibits the rectangular-like and symmetric response of ideal capacitive behaviour, which means that there is a small electric double-layer capacitance in the CNT electrode. For the PANI nanofiber and PANI/CNT composite cells, redox peaks can be observed. In these CVs, it can be shown that the current passed by the PANI/CNT composite-based device is higher than that of PANI nanofiber, which means that the capacitance of the composite is larger than that of the pure PANI nanofiber. This indicates a synergistic effect from the combined contributions from PANI and CNT. The nanoporous PANI/CNT composite provides a large surface area that allows excellent electrolyte access as well as providing low internal resistance.

The cell assembled with PANI/CNT composite electrodes was subjected to charge–discharge cycling in the voltage range of 0–0.6 V at a constant current of 1.0 A g^{-1} , and its charge–discharge curves are shown in Fig. 6(a). The specific capacitance and Coulombic efficiency of the cell as a function of cycle number are presented in Fig. 6(b). The values of specific capacitance were calculated based on the weight of active materials including the CNT. The cell gives an initial specific capacitance of 575 F g^{-1} , which is higher than the pure polyaniline-based cell (554 F g^{-1} at 1st cycle) over the same voltage range. It should be noted, for comparison, that the specific capacitance of the cell assembled with pure CNT is about 42 F g^{-1} , and thus the sum of the specific capacitances from the contents of PANI and CNT is less than 575 F g^{-1} . The PANI/CNT-based cell therefore shows a synergistic effect of the complementary properties of both components, as explained above. It is also observed that the cycleability of the cell is better than that of the cell assembled with polyaniline. This result suggests that the loss of capacitance of the pure polyaniline cell

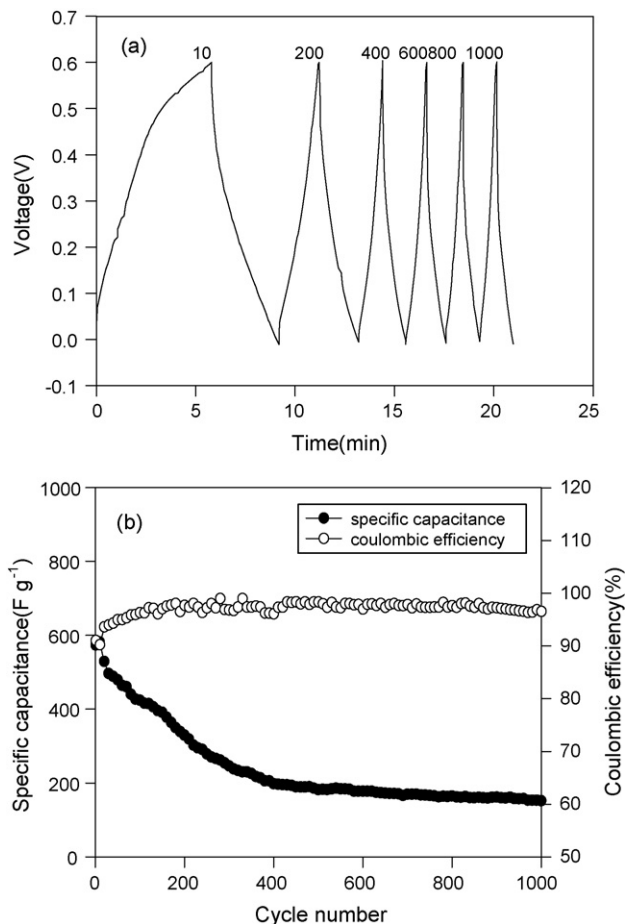


Fig. 6. Cycling performance of PANI/CNT composite-based cell, which is cycled in the voltage range of 0–0.6 V at a current loading of 1.0 A g^{-1} . (a) Charge and discharge curves vs. time and (b) specific discharge capacitance and Coulombic efficiency vs. cycle number.

with cycling is certainly, to some extent, due to the mechanical stress that has been alleviated by the use of CNT support.

The cycling results of the cell assembled with PANI/CNT composite electrodes, which are cycled in voltage range of 0–0.4 V, are presented in Fig. 7. This cell delivers a very high initial specific capacitance of 606 F g^{-1} , and there is no large IR drop even in the last cycle. After 200 cycles, the capacitance experiences a smooth fading and becomes 386 F g^{-1} at the 1000th cycle. On comparing the data in Figs. 6b and 7b, the cell cycled in the range of 0–0.4 V is seen to exhibit better cycleability. This is consistent with the previous results obtained in the PANI nanofiber-based cell.

To gain some insight in the degradation behaviour of the PANI/CNT composite electrodes, the AC impedance of the cells was measured. Fig. 8 presents AC impedance spectra of the cell before cycling, and after 1000 cycles in the voltage ranges of 0–0.4 and 0–0.6 V. All the impedance measurements were made on cells in their discharged state without applying any external potential. In all the three spectra, the cell displays a semicircle followed by a capacitive spike. The capacitive behaviour of the cells is found to start around a frequency of 0.55, 0.48 and 0.37 Hz, respectively. The lowest value in the cell cycled in the voltage range of 0–0.6 V is due to the slow charge and

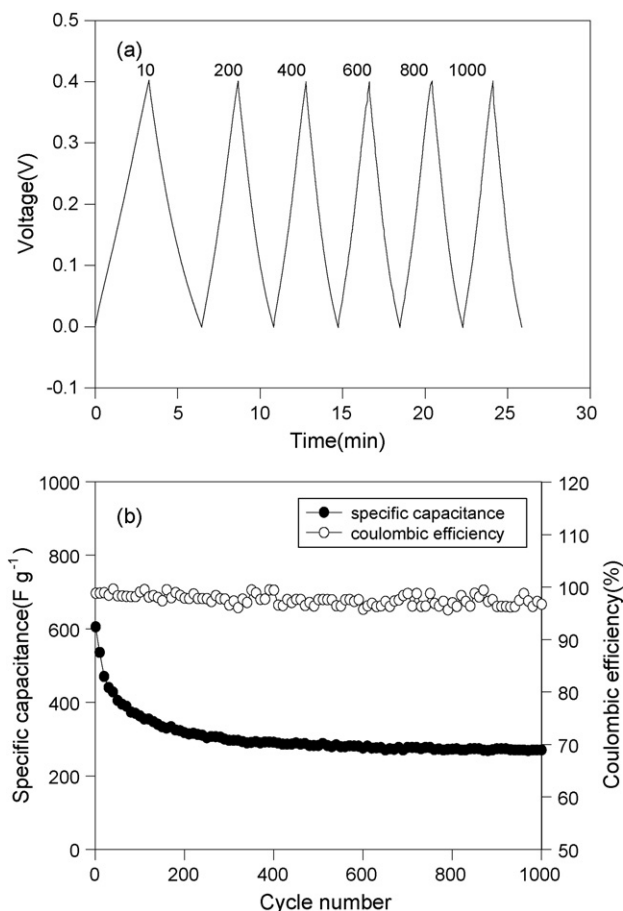


Fig. 7. Cycling performance of PANI/CNT composite-based cell, which is cycled in the voltage range of 0–0.4 V at a current loading of $1.0 A g^{-1}$. (a) Charge and discharge curves vs. time and (b) specific discharge capacitance and Coulombic efficiency vs. cycle number.

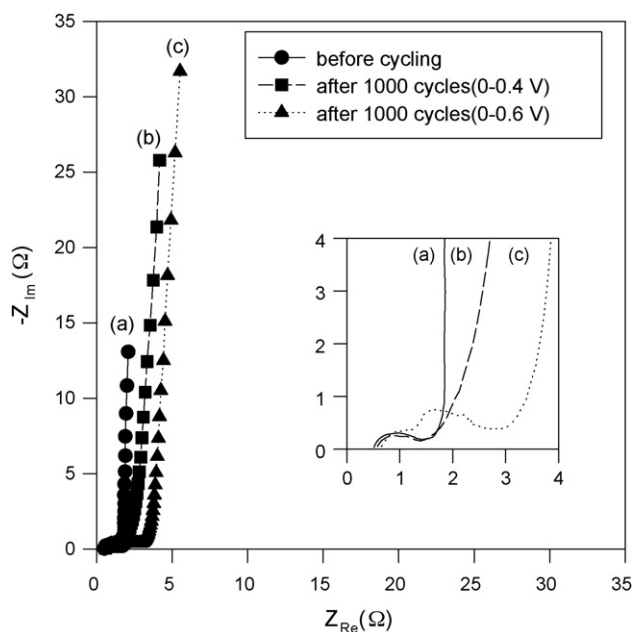


Fig. 8. AC impedance spectra of cells assembled with PANI/CNT composite: (a) before cycling, (b) after 1000 cycles in the voltage range of 0–0.4 V and (c) after 1000 cycles (0–0.6 V).

discharge processes. At high frequencies, the corresponding intercepts with the real axis are 0.51, 0.57 and 0.65 Ω . This intercept is known to be related to the uncompensated electrical resistance of the active materials (R_{Ω}), the electrolyte resistance (R_e) and the electrical leads (R_l) [28]. As R_e and R_l are almost the same, the increase of the intercept is due to an increase in the electrical resistance of the active materials in the cell cycled in the voltage range of 0–0.6 V. As described earlier, a higher cut-off voltage for charging may degrade the polyaniline electrode, which will result in a gradual decrease in its electronic conductivity. In the cell cycled in the range of 0–0.6 V, two semicircles are observed. The reasons for this phenomenon are not clearly understood at this stage, but it is plausible that the second semicircle that appears at a lower frequency is related to another type of charge-transfer reaction that occurs after polymer degradation. Of particular interest in the AC impedance spectra is the total charge-transfer resistance (R_{ct}). The charge-transfer resistances calculated from these spectra are 0.79, 0.81 and 2.24 Ω , respectively. The higher value of R_{ct} in the 0.6 V cell can be ascribed to degradation of the electrode upon cycling. From these results, it can be said that the charging potential can be the important factor in determining the cycling behaviour of the redox supercapacitor assembled with polyaniline-based electrodes.

4. Conclusions

PANI nanofibres have been synthesized and evaluated as an electrode material for aqueous redox supercapacitor. The nanofibres deliver an initial specific capacitance of $554 F g^{-1}$ in the two-electrode cell using 1.0 M H_2SO_4 at a current loading of $1.0 A g^{-1}$. Its capacitance decreases rapidly on continuous cycling, due to both polymer degradation and mechanical stress on the polyaniline. In order to improve the cycleability, a composite of PANI with multi-walled CNTs is synthesized by *in situ* chemical polymerization. The cell assembled with PANI/CNT composite electrodes shows a high initial specific capacitance of $606 F g^{-1}$ and good capacitance retention in the voltage range of 0–0.4 V. Both the specific capacitance and the cycleability for the redox supercapacitor are found to depend on the charging potential.

Acknowledgment

This work was supported by the Korea Research Foundation Grant (KRF-2006-013-D00210).

References

- [1] A. Rudge, J. Davey, I. Raistrick, S. Gottesfeld, J.P. Ferraris, J. Power Sources 47 (1994) 89.
- [2] S. Sarangapani, B.V. Tilak, C.-P. Chen, J. Electrochem. Soc. 143 (1996) 3791.
- [3] D. Belanger, X. Ren, J. Davey, F. Uribe, S. Gottesfeld, J. Electrochem. Soc. 147 (2000) 2923.
- [4] K.S. Ryu, K.M. Kim, N.-G. Park, Y.J. Park, S.H. Chang, J. Power Sources 103 (2002) 305.
- [5] J.H. Park, O.Ok. Park, J. Power Sources 111 (2002) 185.

- [6] K.R. Prasad, N. Munichandraiah, J. Power Sources 112 (2002) 443.
- [7] V. Gupta, N. Miura, Mater. Lett. 60 (2006) 1466.
- [8] T.C. Girija, M.V. Sangaranarayanan, J. Power Sources 156 (2006) 705.
- [9] K. Jurewicz, S. Delpeux, V. Bertagna, F. Beguin, E. Frackowiak, Chem. Phys. Lett. 347 (2001) 36.
- [10] M.D. Ingram, H. Staesche, K.S. Ryder, Solid State Ionics 169 (2004) 51.
- [11] K.S. Ryu, Y.G. Lee, Y.S. Hong, Y.J. Park, X. Wu, K.M. Kim, M.G. Kang, N.G. Park, S.H. Chang, Electrochim. Acta 50 (2004) 843.
- [12] K. Lota, V. Khomenko, E. Frackowiak, J. Phys. Chem. Solids 65 (2004) 295.
- [13] C. Arbizzani, M.C. Gallazzi, M. Mastragostino, M. Rossi, F. Soavi, Electrochem. Commun. 3 (2001) 16.
- [14] M. Mastragostino, C. Arbizzani, F. Soavi, Solid State Ionics 148 (2002) 493.
- [15] K.R. Prasad, N. Munichandraiah, J. Electrochem. Soc. 149 (2002) A1393.
- [16] W.-C. Chen, T.-C. Wen, H. Teng, Electrochim. Acta 48 (2003) 641.
- [17] V. Gupta, N. Miura, Electrochem. Solid State Lett. 8 (2005) A630.
- [18] F. Fusalba, P. Gouerec, D. Villers, D. Belanger, J. Electrochem. Soc. 148 (2001) A1.
- [19] K.S. Ryu, K.M. Kim, Y.J. Park, N.-G. Park, M.G. Kang, S.H. Chang, Solid State Ionics 152 (2002) 861.
- [20] K.S. Ryu, Y. Lee, K.-S. Han, Y.J. Park, M.G. Kang, N.-G. Park, S.H. Chang, Solid State Ionics 175 (2004) 765.
- [21] J. Huang, S. Virji, B.H. Weiller, R.B. Kaner, J. Am. Chem. Soc. 125 (2003) 314.
- [22] M. Gao, S. Huang, L. Dai, G. Wallace, R. Gao, Z. Wang, Angew. Chem. Int. Ed. 39 (2000) 3664.
- [23] Y.-K. Zhou, B.-L. He, W.-J. Zhou, J. Huang, X.-H. Li, B. Wu, H.-L. Li, Electrochim. Acta 49 (2004) 257.
- [24] V. Khomenko, E. Frackowiak, F. Beguin, Electrochim. Acta 50 (2005) 2499.
- [25] V. Mottaghitalab, G.M. Spinks, G.G. Wallace, Synth. Met. 152 (2005) 77.
- [26] M. Baibarac, P. Gomez-Romero, J. Nanosci. Nanotech. 6 (2006) 1.
- [27] E. Frackowiak, V. Khomenko, K. Jurewicz, K. Lota, F. Beguin, J. Power Sources 153 (2006) 413.
- [28] C.J. Wen, C. Ho, B.A. Boukamp, I.D. Raistrick, W. Weppner, R.A. Huggins, Int. Met. Rev. 26 (1981) 253.